

Enhanced Removal of Cr(VI) from Aqueous Solutions Using Poly(Pyrrole)-*g*-Poly(Acrylic Acid-co-Acrylamide)/Fe₃O₄ Magnetic Hydrogel Nanocomposite Adsorbent



doi: 10.15255/CABEQ.2018.1306

H. Hosseinzadeh* and M. M. Tabatabai Asl
Chemistry Department, Payame Noor University,
19395-4697, Tehran, Iran

Original scientific paper
Received: February 21, 2018
Accepted: March 16, 2019

In the present work, the structural characterization and chromium adsorption behavior of a novel poly(pyrrole)-based magnetic hydrogel nanocomposite (MHN) is reported. This product was prepared using free-radical copolymerization of pyrrole (Py), acrylic acid (AA) and acrylamide (AM) monomers, and subsequent *in situ* synthesis of magnetic Fe₃O₄ nanoparticles. The structure of MHNs was then characterized by FTIR, SEM, TEM, XRD, UV-Vis and VSM techniques, and a mechanism for the preparation of MHNs is also proposed. The maximum Cr(VI) adsorption capacity (208 mg g⁻¹) was achieved under the optimum conditions that were found to be: AA = 0.25 mol L⁻¹, AM = 1.2 mol L⁻¹, agitation time = 90 min, solution pH = 1.0, ion concentration = 100 mg L⁻¹, adsorbent dose = 50 mg, and temperature = 65 °C. Further, the calculated values of the thermodynamic parameters ($\Delta H^\circ = 31.33 \text{ kJ mol}^{-1}$, $\Delta S^\circ = 105.67 \text{ J K}^{-1} \text{ mol}^{-1}$, $\Delta G^\circ = -61.33 \text{ kJ mol}^{-1}$) revealed that ion adsorption is a spontaneous and endothermic process. In general, the results indicated that the synthesized MHNs with specific properties can be used in wastewater treatment applications.

Keywords:

hydrogel, nanocomposite, swelling behavior, adsorption

Introduction

In developing countries, water pollution has been emphasized as one of the major threats from the environmental and human health points of view.¹ The non-biodegradable heavy metals are the major sources of water pollution owing to their high toxicity and bioaccumulation in the food chain.² Most of the heavy metal pollutants originate from discharged wastewaters of industries, such as the mining, glass, cement, ceramics, and electroplating industries.³ Among heavy metal pollutants, chromium (Cr) is one of the most toxic heavy metals as reported by the United States Environmental Protection Agency (US-EPA).⁴

In aqueous solutions, Cr exists mainly in two oxidation states, i.e., Cr(III) and Cr(VI). Compared with Cr(III), Cr(VI) is a very toxic ion due to its carcinogenicity and teratogenicity.^{5,6} The allowable limit for Cr(VI) in potable water set forth by US-EPA is 0.05 mg L⁻¹,⁷ while discharged effluents from industries often contain values higher than the mentioned amount. Thus, it is necessary to remove

the Cr(VI) from effluents before discharging them into the environment. To date, various technologies have been explored to reduce Cr(VI) concentrations from aqueous solutions, such as adsorption,^{8–12} ion exchange,^{13,14} membrane process,^{15,16} chemical coagulation,^{17–19} electrochemical reduction^{20,21} and precipitation.²² Of these methods, adsorption is a versatile and eco-friendly method. It is feasible, flexible, effective, simple, and also easy to handle.^{23,24}

In previous studies, different adsorbents were fabricated for removing Cr(VI) from aqueous solutions, such as activated carbon,^{25,26} metal oxides,^{27,28} coated silica gel,²⁹ graphene,³⁰ agriculture waste^{31,32} and biomaterials.^{32–34} However, most of these adsorbents have low adsorption capacity and take a long time to achieve equilibrium adsorption, with poor regeneration possibility of adsorbents for reuse.³⁶

Recently, several researchers have shown interest in nanostructured adsorbents with high adsorption capacities and rapid sorption rates. This is due to the very large surface area, accessible active surface sites, and a short diffusion route of nano-adsorbents.³⁷ However, most nano-adsorbents have some limitations in separating the adsorbents from a large volume of environmental samples. In order to avoid this problem, nano-adsorbents with magnetic prop-

*Corresponding author: E-mail: h_hosseinzadeh@pnu.ac.ir
Tel. +98 44 33855100; Fax: +98 44 33855100

erties have recently received attention for the adsorption of heavy metals from aqueous solutions,^{38,39} because of their magnetic characteristics that lead to higher removal efficiency in a short period.⁴⁰ Various magnetic superabsorbent hydrogel nanocomposites have been synthesized for providing efficient and cost-effective treatment of wastewaters. In this regard, magnetic-based nanostructured materials have been used in the fields of separation and adsorption, because they produce no contaminants, and are capable of treating large amounts of wastewater within a short time. Furthermore, their unique properties allow the target molecules to be separated easily from the matrix by applying an external magnetic field.⁴² In conclusion, no centrifugation or filtration of the sample is needed after treatment (in comparison with non-magnetic adsorbents). Among various nanoparticles, magnetic iron oxide nanoparticles (MIONs) have received considerable attention.⁴³ The large specific surface area, good mechanical stability, high selectivity, easy preparation method, and more active sites, render nanomaterials excellent materials in the treatment of contaminated wastewater.⁴⁴ In summary, nanomaterials can be used as economical materials for the revolution of wastewater treatment applications.

Conducting polymers have attracted increasing attention as a new interdisciplinary field of research for the removal of toxic heavy metals.^{40,45,46} Poly(pyrrole), poly(aniline), and poly(thiophene) are popularly used as conducting polymer adsorbents due to their non-toxicity, low cost, good environmental stability, and ease of preparation.^{47–50} Among the family of conducting polymers, poly(pyrrole) and its composite have been proven to be good adsorbents for the removal of Cr(VI).^{51,52} This is due to the excellent redox properties, high thermal stability, non-toxicity, good biocompatibility, high electrical conductivity, relatively low cost, facile preparation, and the existence of positively charged nitrogen atoms in poly(pyrrole) matrix.^{52–56} These properties lead to a higher adsorption ability through ion exchange or electrostatic interactions.

In previous studies, different adsorbents have been fabricated for the removal of various heavy metals. However, most of the previously reported adsorbents have relatively low Cr adsorption capacity. Therefore, it is necessary to search for highly abundant, low cost adsorbents with greater adsorption capacity in order to remove Cr(VI) ions from contaminated water. Hence, the main goal of the present study is to fabricate a novel adsorbent with high removal efficiency through simple polymerization process for removal of Cr(VI) ions from aqueous solutions. Here, the use of poly(pyrrole) substrate with unique properties, as well as radical polymerization method with special advantages was

regarded as the novelty of the synthesized adsorbent. We report *in situ* chemical oxidative synthesis, characterization, and application of poly(pyrrole)-*g*-poly(acrylic acid-*co*-acrylamide)/Fe₃O₄ magnetic hydrogel nanocomposite adsorbent for the removal of Cr(VI) from wastewater with high adsorbent capacity that can be separated magnetically. The ion adsorption behavior of adsorbent along with the thermodynamics and kinetics of adsorption were studied in detail.

Experimental part

Materials

Pyrrole (Py, 98 %) was purchased from Merck, and distilled twice under reduced pressure. Py was then stored in the dark under nitrogen prior to use. Ammonium persulfate (APS, from Fluka), *N,N'*-methylene bisacrylamide (MBA, from Merck), ferric chloride hexahydrate (FeCl₃·6H₂O, from Merck), ferrous chloride tetrahydrate (FeCl₂·4H₂O, from Merck), and ethylenediamine were used as received. Acrylic acid (AA, from Merck) was used after vacuum distillation. Acrylamide (AM, from Fluka) was used after crystallization in acetone. In addition, potassium dichromate (K₂Cr₂O₇) was obtained from Sigma-Aldrich, USA. Finally, the solution (1000 mg L⁻¹) of Cr(VI) was prepared by dissolving 2.83 mg of K₂Cr₂O₇ in 1 L of doubly-distilled water. All other chemicals used in this study were commercially available and used directly without further purification. All required solutions were prepared with distilled water.

Preparation of MHN adsorbent

For the synthesis of Py-based MHN adsorbents, monomers (acrylic acid 2.0 mL and acrylamide 2.0 g) were added to a three-neck reactor equipped with a mechanical stirrer (RZR 2021, a three-blade propeller type, Heidolph, Schwabach, Germany), and stirred (300 rpm) for 20 min. The reactor was placed in a water bath preset at 60 °C. Then, 5.0 mL of Py solution (2.0 g of Py dissolved in 5 mL of 1:1 water/ethanol) was added to the mixture. After dispersing the monomers and homogenizing the mixture, the initiator APS (0.1 g dissolved in 5 mL H₂O) was added to the reaction mixture. In the next stage, appropriate amounts of FeCl₂·4H₂O (0.3–1.8 mmol) and FeCl₃·6H₂O (0.2–1.2 mmol) with ratio of 2:1 of Fe³⁺/Fe²⁺ were added into the solution. Next, 10 mL of 2 M NH₄OH and crosslinker MBA (0.05 g dissolved in 5 mL H₂O) was dropped gradually into the mixture with vigorous stirring until completion of the polymerization process (3 h). A black material was precipitated immediately and collected by a

ceramic block magnet. The as-prepared adsorbent was finally washed with ultra-pure deionized water three times, and dried at 70 °C for 10 h in vacuum oven. It should be noted that the APS acts both as an initiator and an oxidant for free-radical polymerization of acrylic monomers and Py monomer.

Characterization of MHN adsorbent

A FTIR spectrophotometer (Quebec, Canada) was used to record the spectra at 500–4000 cm^{-1} by KBr pellets. The fractured morphology of the gel was examined using scanning electron microscopy (SEM, Leo 1455 VP) at 30 kV acceleration voltage. Dried MHN powders were coated with 3 nm thin layer of palladium gold alloy. The software used for SEM imaging was SEM ODon. Transmission electron microscopy (TEM) micrographs were recorded with a Philips CM10 (UK) operating at voltage of 60 kV. The TEM analysis was also carried out by the Microstructure Measurement and NemoDar software. The X-ray diffraction (XRD) patterns of samples were also recorded using a Siemens D-500 X-ray diffractometer with wavelength $\lambda = 1.54 \text{ \AA}$ (Cu-K α). Thermogravimetric analyses (TGA) were performed on a Universal V4.1D TA Instruments (SDT Q600) under nitrogen atmosphere, and at a heating rate of 10 °C min^{-1} . The magnetization was measured at 25 °C with a vibrating sample magnetometer (VSM; Model 7400, Lakeshore Company, USA).

Swelling measurements of MHN adsorbent

An accurately weighed sample of the powdered MHN ($0.1 \text{ g} \pm 0.001$), with average particle sizes between 250–350 μm , was immersed in distilled water (200 mL) or pH solution (100 mL), and allowed to soak for 3 h at room temperature. The equilibrium swelling (ES) capacity was measured twice at room temperature according to a conventional tea bag method using the following formula:

$$\text{ES}(\text{g g}^{-1}) = \frac{\text{Weight of swollen gel} - \text{Weight of dried gel}}{\text{Weight of dried gel}} \quad (1)$$

Desorption and regeneration of MHN adsorbent

For evaluating the reusability of the nanocomposites, a weighed sample of the MHN, swollen in pH 3.0 or pH 9.0, was placed in 200 mL of ethanol and agitated at room temperature for 60 min. The de-swollen sample was then separated from the solution using the tea bag method, washed with ethanol, and finally dried in an oven at 60 °C for reuse in the subsequent four runs.

Chromium adsorption experiments

Batch adsorption experiments were performed for the removal process in a pH 6.0 solution at 25 °C. Typically, 10 mg of MHN adsorbent was added to 50 mL of Cr(VI) aqueous solution (100 mg L^{-1}) in glass vials placed in a controlled-temperature shaking water bath operating at 300 rpm. After the adsorption process, the Cr(VI)-loaded MHN adsorbents were separated magnetically from solution with a magnet, and the supernatant was analyzed immediately via atomic absorption spectrometry measurement of the sample solution before and after the removal process. The amount of Cr(VI) ions adsorbed on the adsorbents was calculated based on the difference in the Cr(VI) concentrations, using the following equation:

$$q_e = \frac{(\gamma_0 - \gamma_e) \cdot V}{m} \quad (2)$$

where q_e (mg g^{-1}) is the equilibrium amount of adsorbed ions, γ_0 (mg L^{-1}) is the initial Cr(VI) concentration, γ_e (mg L^{-1}) is the concentration of Cr(VI) at equilibrium, V (L) is the solution volume, and m (g) is the mass of the adsorbent.

Results and discussion

Mechanism of MHN adsorbent preparation

Fig.1 shows a simple and general schematic illustration of the preparation of MHN product. In the first step, the thermally dissociating initiator and oxidant, *i.e.*, ammonium persulfate, was decomposed under heating (60 °C) to produce sulfate anion radicals. The produced radicals initiate the polymerization of acryl amide (AM) and acrylic acid (AA), as well as oxidation of Py monomer, leading to formation of poly(Py)-based graft copolymer. The iron salts were then added to the mixture. In this step, the free $-\text{NH}_2$ and $-\text{COOH}$ groups of grafted PAM and PAA formed chelating sites with Fe^{2+} and Fe^{3+} ions. By simultaneous addition of NH_4OH and MBA, the formation of Fe_3O_4 and cross-linking points were completed, which resulted in uniform growth and dispersion of magnetic nanoparticles, and stabilization of the synthesized magnetic superabsorbent nanocomposites.

Characterization of MHN adsorbent

Regarding the characterization, the FTIR spectra of poly(Py) hydrogel, poly(AA-co-AM) hydrogel, poly(AA-co-AM)/ Fe_3O_4 hydrogel, and poly(Py)-g-poly(AA-co-AM)/ Fe_3O_4 magnetic hydrogel nanocomposite adsorbent were recorded (Fig. 2). In the FTIR spectrum of poly(Py) hydro-

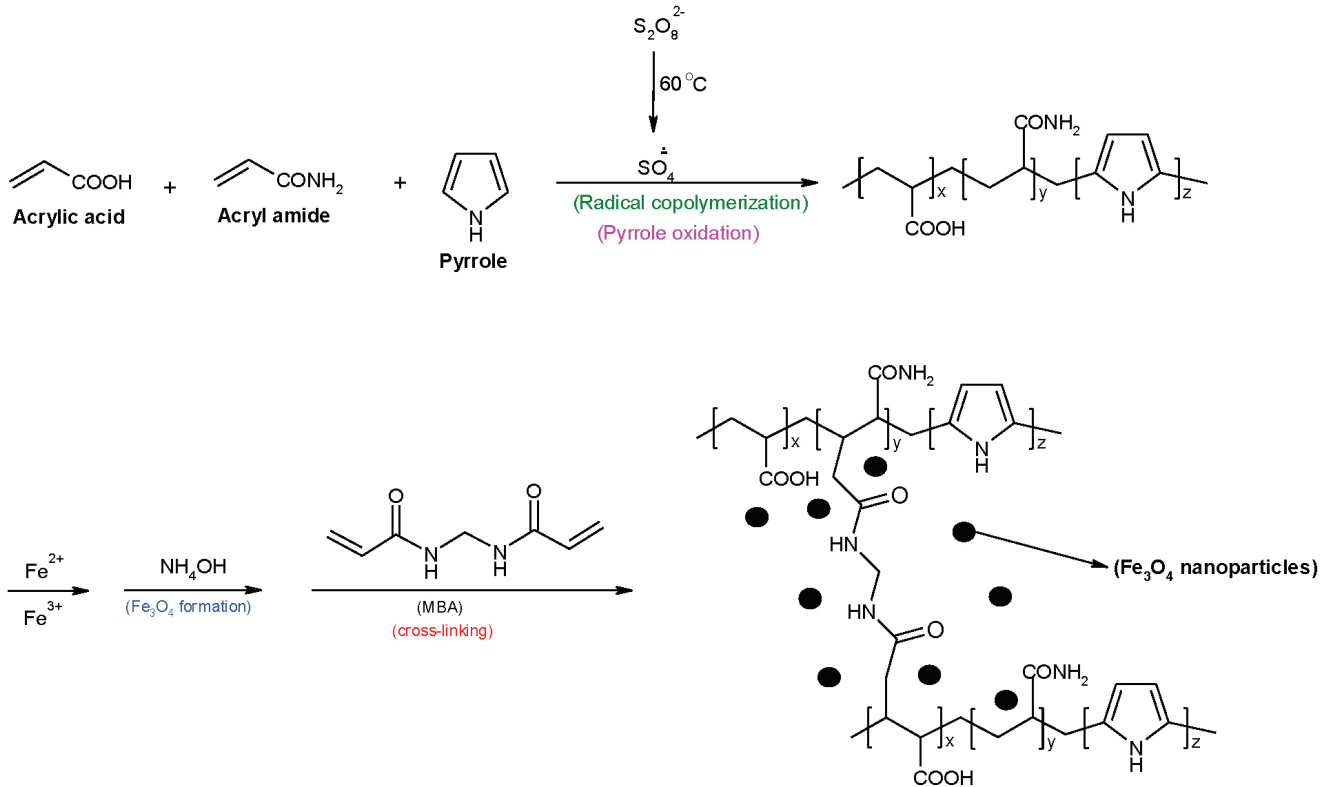
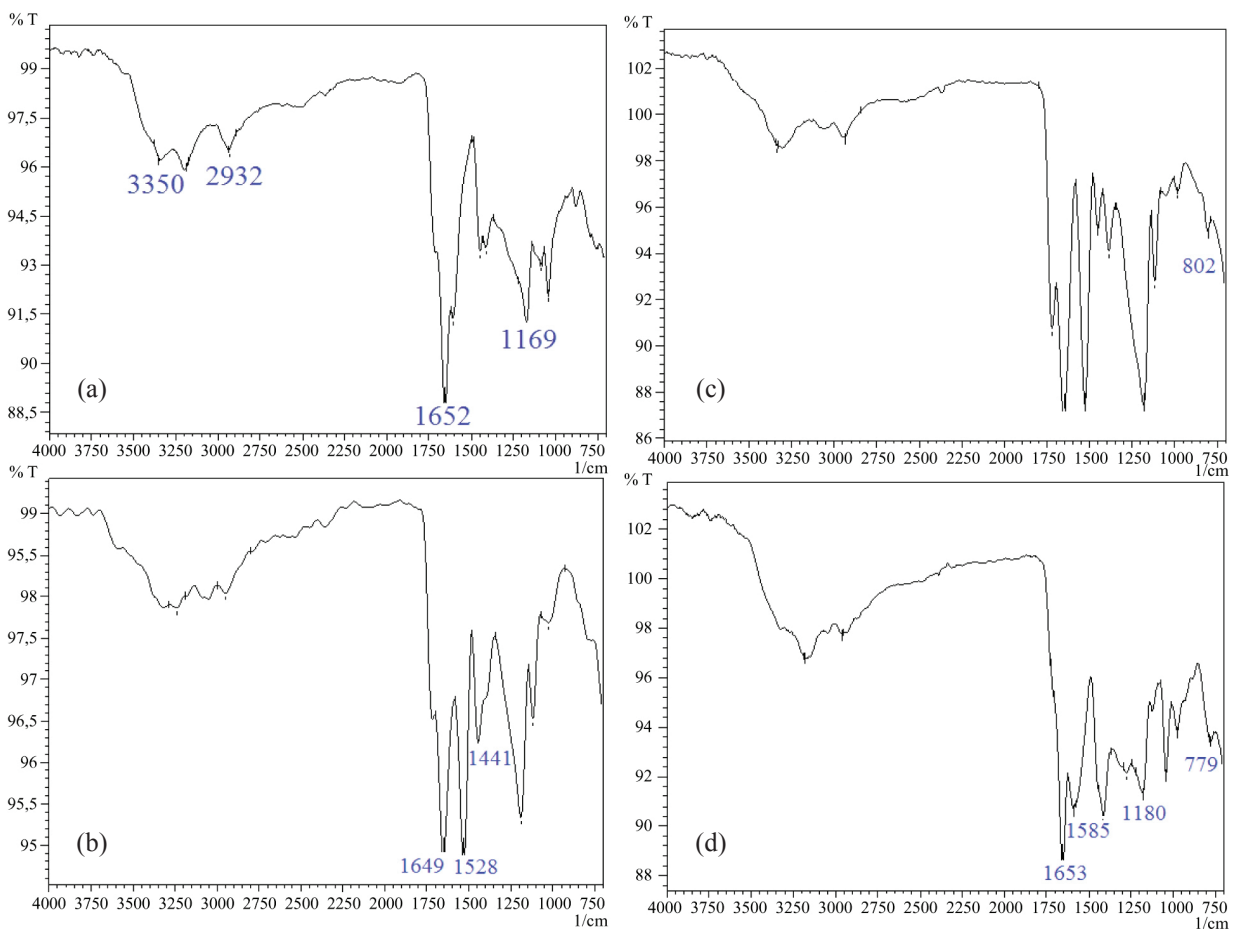


Fig. 1 – Proposed mechanistic pathway for the synthesis of MHN adsorbent

Fig. 2 – FTIR spectra of poly(Py) hydrogel (a), poly(AA-co-AM) hydrogel (b), poly(AA-co-AM)/ Fe_3O_4 hydrogel (c), and MHN adsorbent (d)

gel, the peaks observed at 1169 and 3350 cm^{-1} can be attributed to the bending and stretching vibrations of N–H band in pyrrole structure, respectively (Fig. 2(a)). Moreover, the wavenumbers 1652 and 2932 cm^{-1} may be assigned to the stretching vibration of C=C and C_{sp^3} -H bands of pyrrole ring. The spectrum of poly(AA-co-AM) hydrogel shows three peaks at 1441, 1528 and 1649 cm^{-1} , which are related to the symmetric and asymmetric vibrations of carboxylate and carbonyl functional groups (Fig. 2(b)). In the FTIR spectrum of poly(AA-co-AM)/ Fe_3O_4 hydrogel (Fig. 2(c)), the new peak at 802 cm^{-1}

is attributed to the adsorbing characteristics of Fe_3O_4 nanoparticles (Fe–O band). Finally, in the FTIR spectrum of MHN adsorbent (Fig. 2(d)), the intensity and position of all bands had changed to some extent, due to interactions of various functional groups with Fe_3O_4 nanoparticles.

The SEM images of normal hydrogel, poly(Py)-g-poly(AA-co-AM), and magnetic hydrogel nano-composite adsorbent, poly(Py)-g-poly(AA-co-AM)/ Fe_3O_4 , are shown in Fig. 3. The SEM images of normal hydrogel demonstrate a flat and smooth surface. After *in situ* insertion of Fe_3O_4 nanoparticles

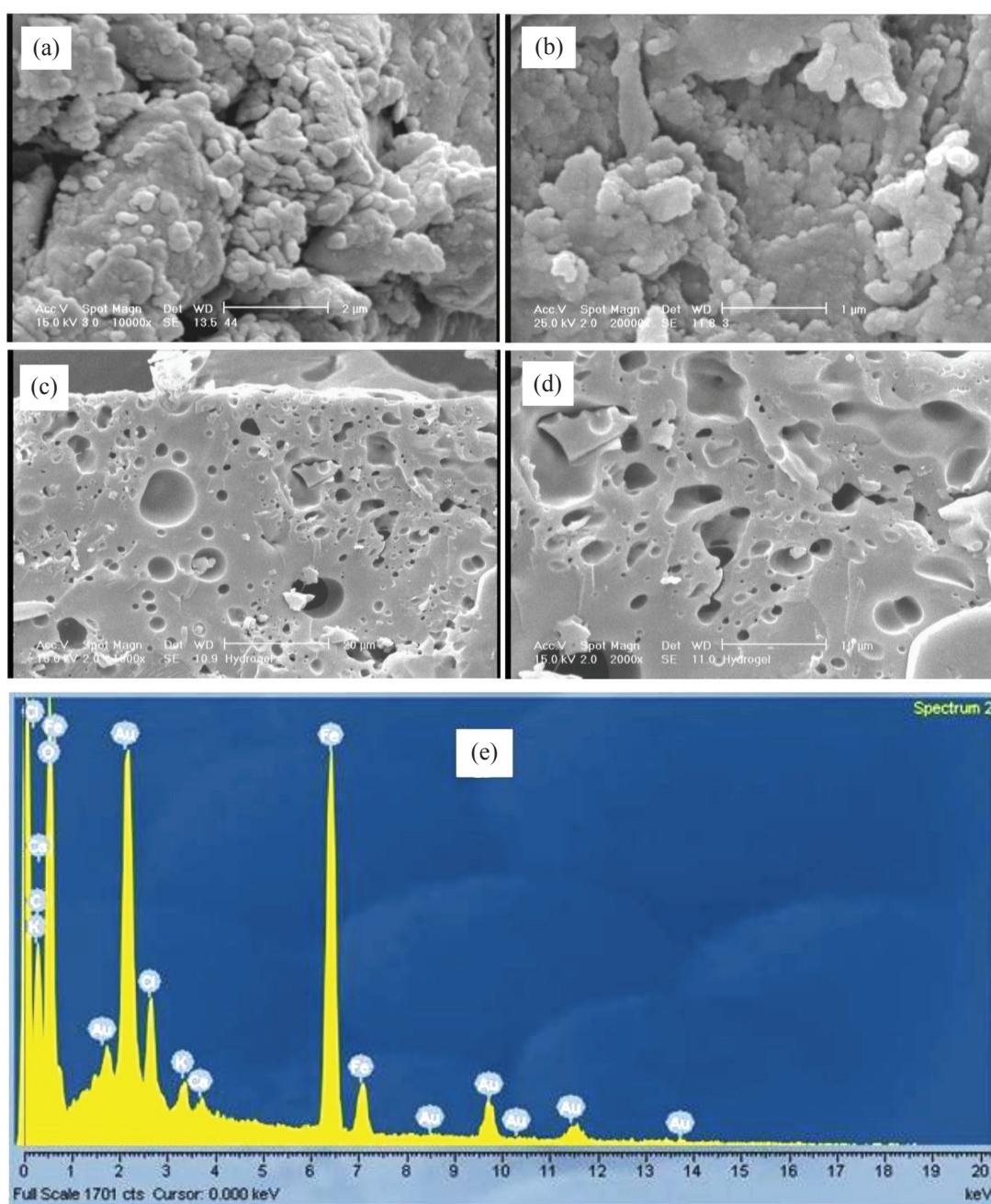


Fig. 3 – SEM images of poly(AA-co-AM)/ Fe_3O_4 hydrogel (a and b) and MHN adsorbent (c and d) with different magnification. The EDS spectra of MHN adsorbent (e).

into the hydrogel network structure, the nanoparticles were successfully deposited on the surface of polymer (Fig. 3(c and d)). Additionally, the structure of MHN adsorbent with considerable amount of pores can be seen clearly, which were appropriate sites for Cr(VI) adsorption process. It should be noted that the MHN has a large surface area, and thus there is a capability of fast swelling and ions being absorbed into these pores and surfaces. Corresponding to SEM images, the energy dispersive spectrum (EDS) analysis of the prepared MHN adsorbent (Fig. 3(e)) displays main signals for the product (*i.e.*, carbon, oxygen, and iron), which confirms the formation of Fe_3O_4 nanoparticles in the adsorbent. The presence of carbon and oxygen in the EDS spectrum is related to pyrrole and acrylic monomers. Moreover, the presence of Au, Cl, and Ca atoms could be due to the presence of the thin layer of palladium gold alloy and the residue of the magnetic hydrogel nanocomposite adsorbent.

The morphology of magnetic adsorbent was also studied by TEM method. As may be seen from Fig. 4, the Fe_3O_4 nanoparticles in the product structure are in the nanometer scale and agglomerated in the adsorbent network due to the hydrogen bonding formation between functional groups of MHN adsorbent and Fe_3O_4 nanoparticles. The related histograms of the Fe_3O_4 nanoparticles are given in Fig. 4. It can be seen that the average diameter of the Fe_3O_4 nanoparticles was approximately 10 nm.

Furthermore, the crystalline structure of the MHN adsorbent was examined using XRD patterns (Fig. 5). The XRD pattern of the MHN was compared with the normal hydrogel. The different peaks at $2\theta = 36, 55$ and 64° in the XRD pattern of the MHN were assigned to Fe_3O_4 nanoparticles incorporated in the nanocomposite network, which correspond to scattering from the (111), (211) and (220) planes, respectively.⁵⁷ Thus, this result further demonstrates that Fe_3O_4 nanoparticles were successfully fabricated in this work. However, it should be noted that the broadened XRD characteristic peaks confirmed that some amorphous phase formed due to the interactions between Fe_3O_4 nanoparticles and functional groups of the MHN adsorbent.

The superparamagnetic property of the MHN adsorbent was determined by vibrating sample magnetometer (VSM) technique. The magnetization curve showed that the synthesized MGON product was superparamagnetic with no coercivity and no remanence at room temperature (Fig. 6). The saturation magnetization of the product was strong enough to separate it from aqueous solution.

The thermogravimetric analysis (TGA) method was also applied to investigate the thermal stability and decomposition pattern of normal hydrogel and magnetic hydrogel nanocomposite, as well as to prove the successful grafting of Fe_3O_4 and acrylic polymers at the surface of poly(pyrrole). As may be seen in Fig. 7, all the samples show a small weight

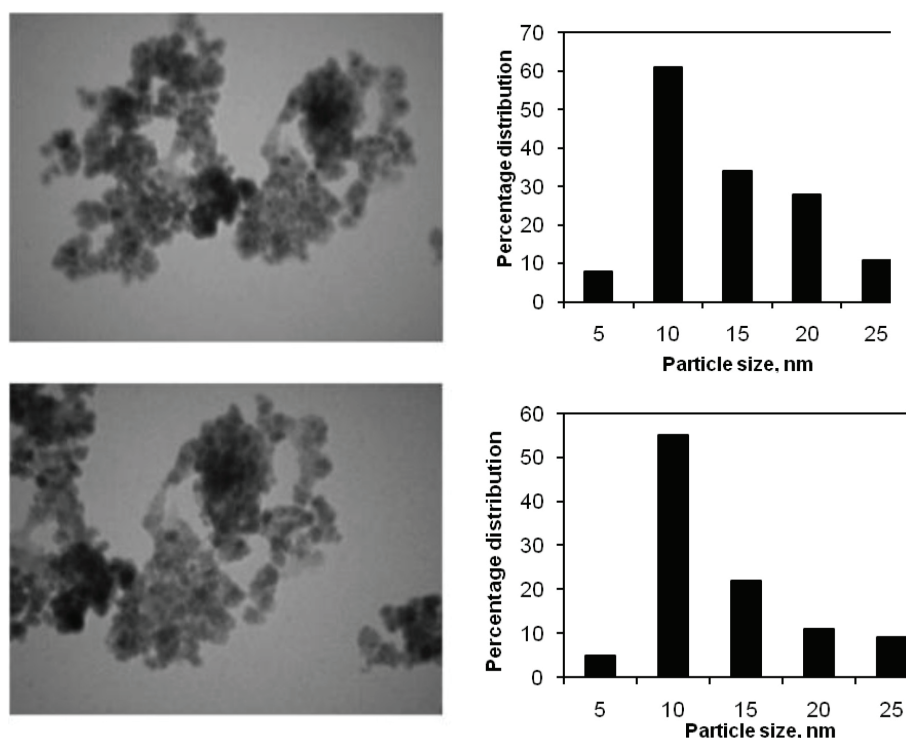


Fig. 4 – TEM images and related histograms of MHN adsorbent

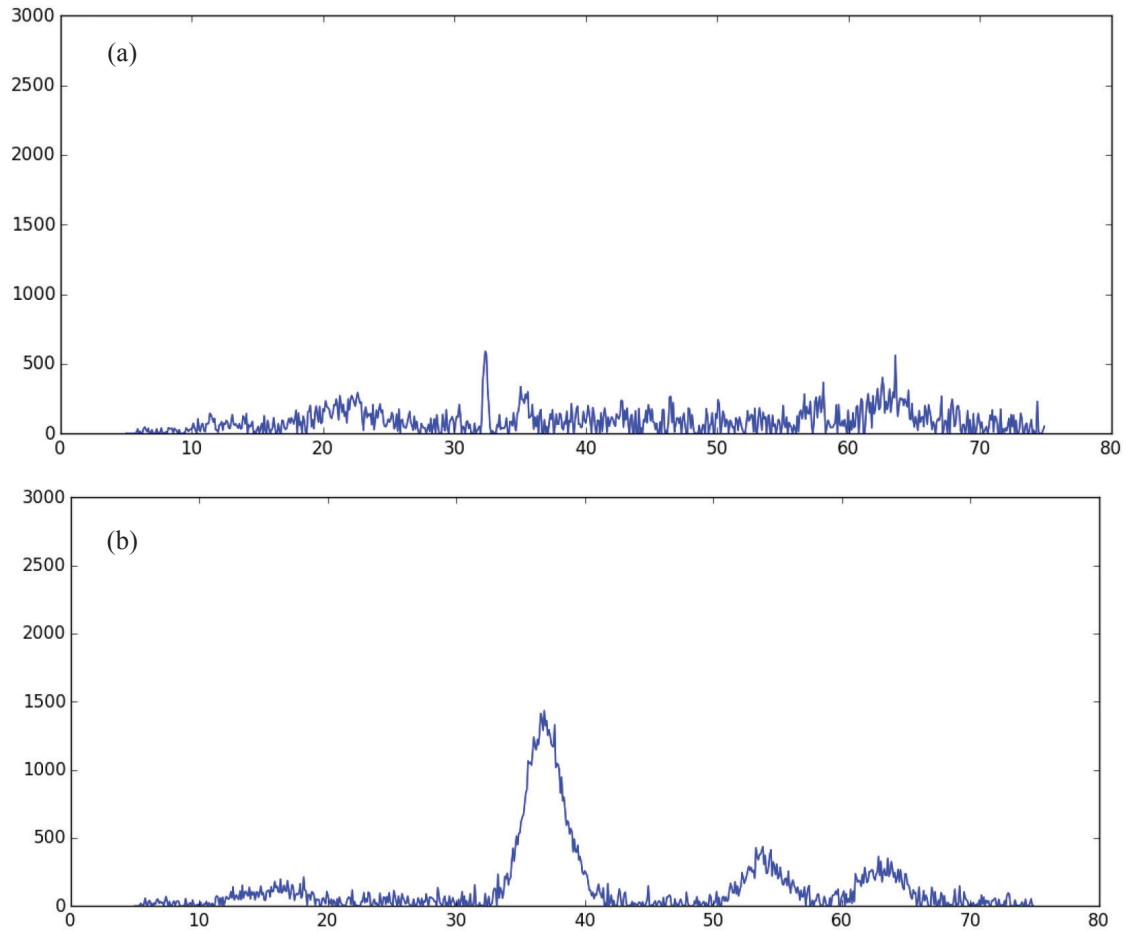


Fig. 5 – XRD pattern of poly(AA-co-AM)/ Fe_3O_4 hydrogel (a) and MHN adsorbent (b)

loss at low temperatures ($<150\text{ }^\circ\text{C}$) as a result of the evaporation of the absorbed moisture on the surface. Furthermore, the final product showed an acceptable thermal stability due to the presence of crosslinking points and Fe_3O_4 nanoparticles within the networks. In detail, the MHN demonstrates three main stages of weight loss with heating. The first one was around 10 % and occurred up to $200\text{ }^\circ\text{C}$, which was due to the removal of adsorbed water. The second weight loss (35 %) may be attributed to the decomposition of graft copolymers backbones and the destruction of the crosslinked polymer chains. Finally, at temperatures above $366\text{ }^\circ\text{C}$, carbonization of polymer occurred and produced a significant amount of residual mass (23 wt%).⁵⁸ Moreover, CO was released at higher temperatures.⁵⁹ In general, the thermal stability of the nanocomposites containing iron nanoparticles was higher than that of the polymers without nanoparticles. The presence of the bonds between polymers and iron nanoparticles prevented the intimate thermal degradation, and conclusively increased the thermal stability of the nanocomposites with Fe_3O_4 nanoparticles.⁶⁰

Effect of magnetic field on swelling behavior of MHN

As shown previously in Fig. 6, the prepared MHNs are capable of responding to an external magnetic field (EMF). Hence, in this series of ex-

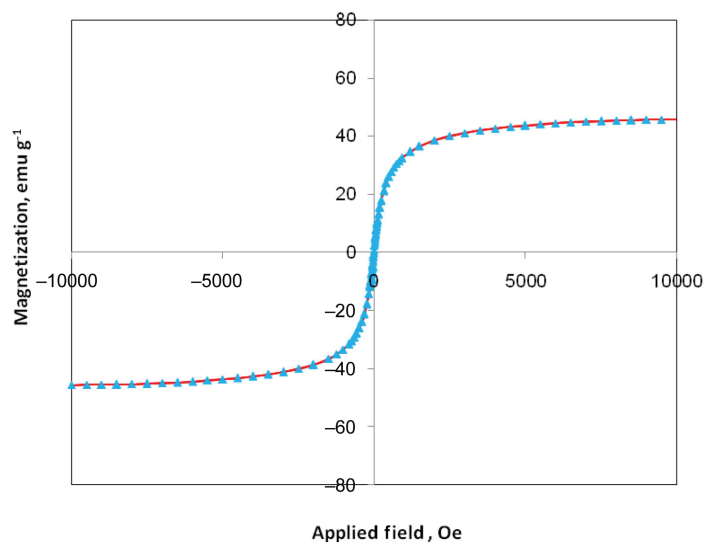


Fig. 6 – Magnetization curve of MHN adsorbent at 298 K

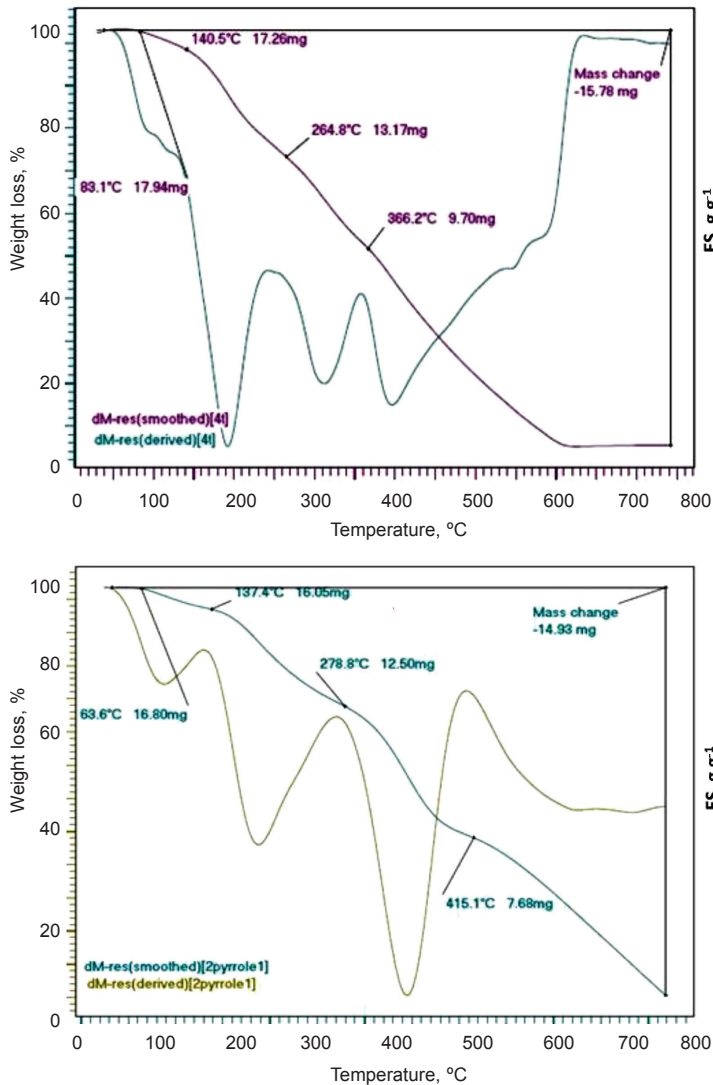


Fig. 7 – Thermogravimetric (TGA/DTG) analysis of (a) poly(AA-co-AM)/Fe₃O₄ hydrogel (S₂) and (b) MHN adsorbent (S₃)

periments, we investigated the effect of an EMF on the swelling capacities of the as-synthesized MHNs (Fig. 8(a)). As may be seen from the figure, the ES of MHN adsorbent is higher in the presence of EMF. This behavior is because the EMF expands the MHN networks and allows more water molecules to diffuse into the nanocomposite structure, resulting in increased swelling capacity.

Furthermore, the MHN adsorbent indicated reproducible swelling-deswelling cycles in the presence and absence of an EMF, as demonstrated in (Fig. 8(b)). As shown in the figure, the magnetic hydrogel nanocomposite swells up to 61 g g⁻¹ in the presence of EMF, while it shrinks within a few minutes in the absence of an EMF upto 7 g g⁻¹. This sudden and sharp swelling-deswelling behavior makes the system highly magnetic-responsive and suitable for tailoring pulsatile (on-off swelling) magnetic-sensitive drug delivery systems.

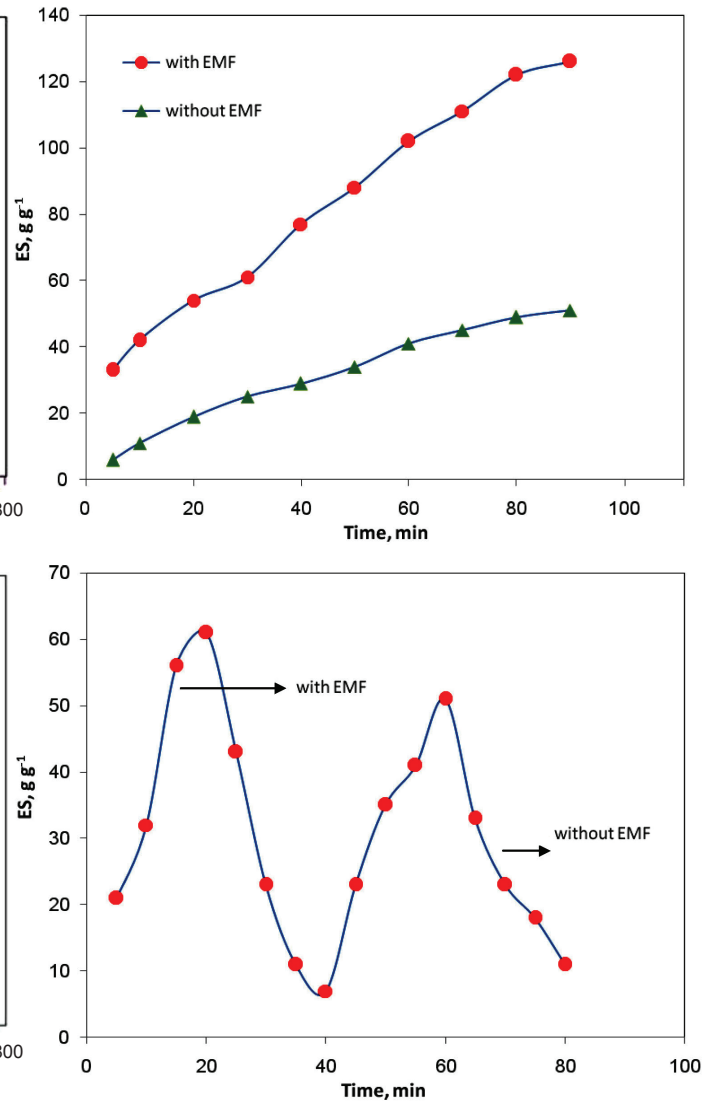


Fig. 8 – Swelling (a) and reproducible swelling-deswelling of MHN adsorbent with and without applying magnetic field (b)

Comparison of swelling behavior

The swelling capacities of four samples, *i.e.*, poly(Py) hydrogel (S₀), poly(AA-co-AM) hydrogel (S₁), poly(AA-co-AM)/Fe₃O₄ hydrogel (S₂), and poly(Py)-g-poly(AA-co-AM)/Fe₃O₄ magnetic hydrogel nanocomposite adsorbent (S₃) were investigated in order to study the swelling behavior in aqueous environments. The feed amounts of components are given in detail in Table 1. The results of swelling capacities and swelling rates are also shown in Fig. 9(a). Firstly, it may be seen that the swelling capacities of the magnetic nanocomposite adsorbent containing Fe₃O₄ nanoparticles (sample S₃) is greater than that of other samples. This might be attributed to the great number of hydrophilic groups and the presence of magnetic nanoparticles synthesized *in situ* on the surface of adsorbents, which resulted in increasing the rate of water diffu-

Table 1 – Feed compositions of the hydrogel samples

Sample	AA (mL)	AM (g)	Py (mL)	APS (g)	MBA (g)	Fe ₃ O ₄ (mg)
S ₀	2	2	1	0.1	0.05	0
S ₁	2	2	0	0.1	0.05	0
S ₂	2	2	0	0.1	0.05	0.5
S ₃	2	2	1	0.1	0.05	0.5

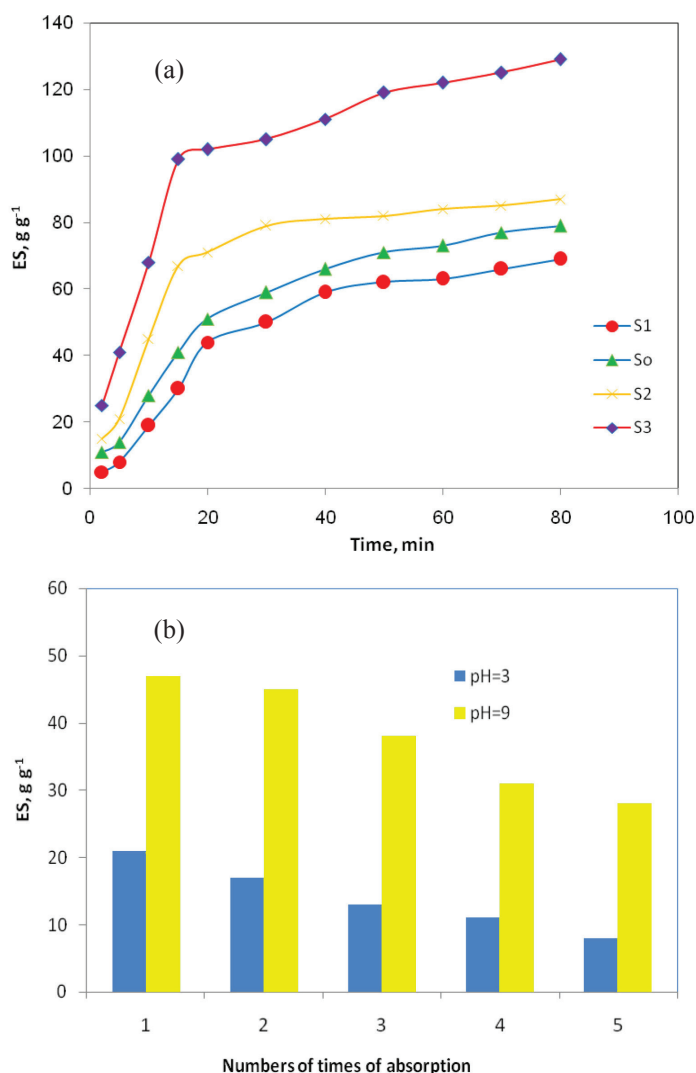


Fig. 9 – Swelling comparison of the hydrogel samples (a) and reversibility behavior of the MHN adsorbent in pH 3.0 and 9.0 at 37 °C

sion in the polymer network (also comparing S₁ and S₀). Further, the ultimate water absorbency of S₀ sample is lower than that of other samples because the pyrrole ring, as a hydrophobic component of network, restricts the adsorption and diffusion of a large quantity of water molecules within the hydrogel structure. Therefore, the order of water absorbency capacity of the samples is S₃>S₂>S₀>S₁.

Swelling desorption and regeneration study

In practical applications, desorption and recycling of adsorbents after removal of water is very important process. For the application of adsorbents on an industrial scale, usually five adsorption-desorption cycles are used. Therefore, in the present work, five cycles of the adsorption-desorption were carried out at pH 3.0 and 9.0 to evaluate the reusability of the MHN adsorbent (Fig. 9(b)). The results indicated that, in the first regeneration cycle, the equilibrium swelling capacity was 49 and 21 g g⁻¹, and after the fifth cycle, it had decreased by 1.75 and 2.6 times at pH 9.0 and 3.0, respectively. Thus, the as-prepared adsorbents can be used as high-performance recyclable materials for industrial applications.^{61,62}

Chromium adsorption of MHN

In the present study, it is expected that the final product can be used as an efficient adsorbent for removal of Cr(VI) ions due to the presence of various functional groups on the structure of the synthesized MHN. To this end, different experimental parameters were varied in order to achieve the best experimental conditions for Cr(VI) adsorption. It is worth noting that the adsorption capacity of a hydrogel network is dependent on the interaction between the adsorbate and the polymer network, the solubility of the adsorbate, and the swelling ratio of hydrogels in aqueous media. In this study, the ion adsorption behavior depended mainly on the attractive interactions and the swelling capacity of the hydrogel. Moreover, the swelling capacity of hydrogels is strongly influenced by their chemical composition. The swelling of adsorbents in water leads to an enhanced removal of adsorbates. In fact, it was observed that the ion adsorption capacity profile of hydrogels was consistent with the data obtained from the swelling studies. The hydrogel with the higher swelling ratio achieved higher adsorption capacity percentages.

Effect of magnetic nanoparticles on chromium adsorption

Fig. 10(a) displays the effect of Fe₃O₄ nanoparticles on the Cr(VI) adsorption capacity of MHN adsorbents. As shown, the ion adsorption capacities improved in the MHN (S₃: with Fe₃O₄ nanoparticles) compared with non-MHN (S₀: without Fe₃O₄ nanoparticles) adsorbent. This behavior was due to an increment in the –OH functional groups content within the structure of MHN adsorbent. In addition, in the presence of Fe₃O₄ nanoparticles, the overall porosity had increased and conclusively led to an increase in the Cr(VI) adsorption capacities of MHN adsorbent.⁶³ According to the figure, the ulti-

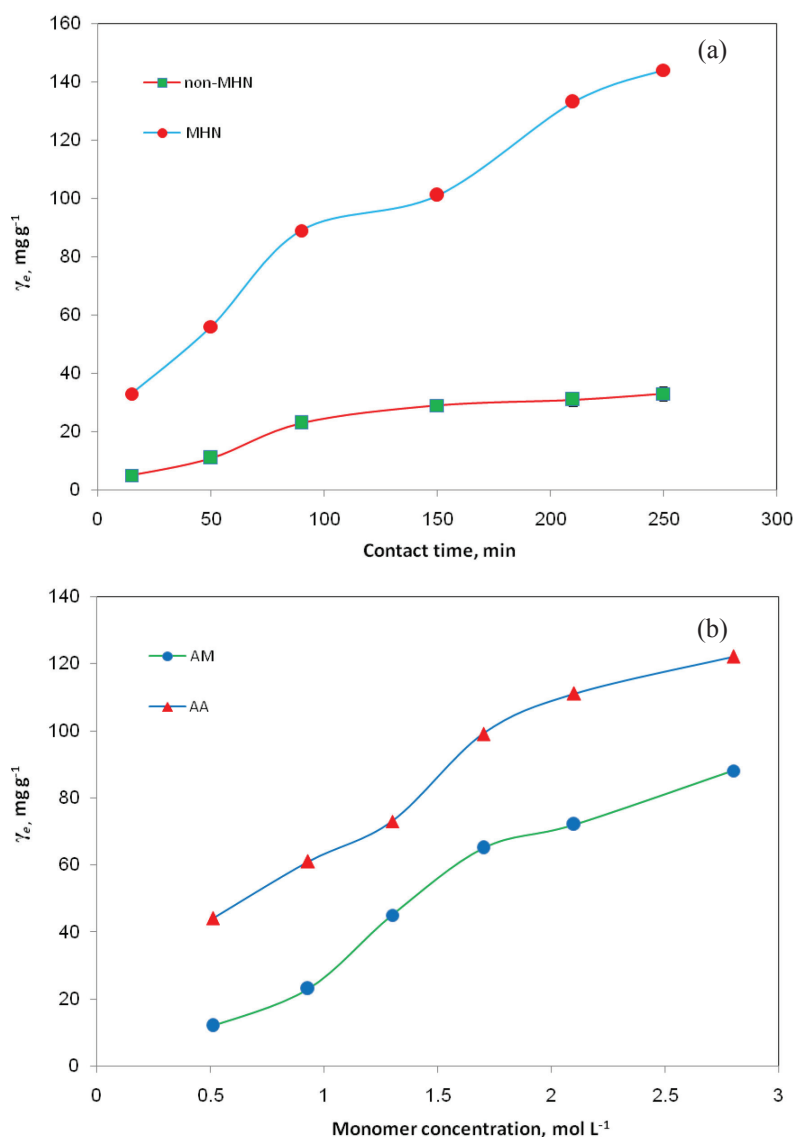


Fig. 10 – Effect of magnetic content (a) and monomer concentrations (b) on Cr(VI) adsorption capacity of MHN adsorbent

mate ion adsorption capacity of MHN and non-MHN are 144 mg g^{-1} and 33 mg g^{-1} , respectively. Thus, the nanoparticles increased the adsorption capacity upto 336 %.

Effect of monomer concentration on chromium adsorption

Fig. 10(b) shows the effect of AA and AM concentration ($0.51\text{--}2.8 \text{ mol L}^{-1}$) on Cr(VI) adsorption of the MHN adsorbent. It may be clearly observed that the diffusion of AA and AM molecules into the polymer structure had increased with the increase in the monomers concentration. Consequently, an increase in functional groups causes an increase in the affinity for more absorption of Cr(VI) ions. Moreover, this leads to an increase in swelling capacity, and therefore the ion adsorption ability of the nanocomposites.

Effect of solution pH on chromium adsorption

In general, the initial pH of solution is one of the most critical parameters that affect the adsorption capacity of an adsorbent extensively.¹² This is because the solution pH changes the surface charge and adsorption sites of an adsorbent. Further, pH is considered an important controlling parameter for any kind of metal adsorption process. According to the literature,³⁶ Cr(VI) exists in the forms of HCrO_4^- and $\text{Cr}_2\text{O}_7^{2-}$ between pH 2–6, while CrO_4^{2-} is the dominant species at pH 6.

The effect of initial solution pH on Cr(VI) adsorption capacities of the MHN adsorbent is shown in Fig. 11(a). As shown, the sorption capacity decreases from 121 mg g^{-1} (at pH 2) to 11 mg g^{-1} (at pH 10). This behavior is related to the competitive interaction between OH^- and CrO_4^{2-} ions at higher pHs ($\text{pH} > 6$). At acidic pHs ($\text{pH} 2\text{--}6$), however, the higher Cr(VI) adsorption efficiency is due to the electrostatic interactions between the positively charged functional groups of the MHN adsorbent and the negatively charged HCrO_4^- and $\text{Cr}_2\text{O}_7^{2-}$ ions.

For further study of the effect of solution pH on the adsorption efficiency of the synthesized adsorbent, the zero-point charge pH (pH_{zpc}) of the MHN was also determined at different pH in the range of 3–11. The results in Fig. 11(b) show that the pH_{zpc} was 6.0. This means that at pH values lower than 6.0, the adsorption sites on MHN adsorbent are positively charged, but at pH values higher than 6.0, the sample surfaces are negatively charged, which could adsorb anions by electrostatic attraction. In other words, the surface of an adsorbent is neutral at $\text{pH} = \text{pH}_{\text{zpc}}$, negatively charged at $\text{pH} > \text{pH}_{\text{zpc}}$, and positive at $\text{pH} < \text{pH}_{\text{zpc}}$. Conclusively, at pH values lower than pH_{zpc} , the MHN adsorbents comprised positively charged functional groups on their surfaces, which provided the best balance with the negative charges of Cr(VI) ions.

Thermodynamics of ion adsorption

We firstly evaluated the effect of different temperatures (25, 45, and 65 °C) on the Cr(VI) adsorption capacity. The results in Fig. 12(a) indicated that the ion adsorption had increased with an increase in solution temperature for various concentrations of ion (50, 100 and 150 mg L^{-1}), which demonstrated that higher temperatures were more suitable for the adsorption process. This means that the ion adsorption process is endothermic.

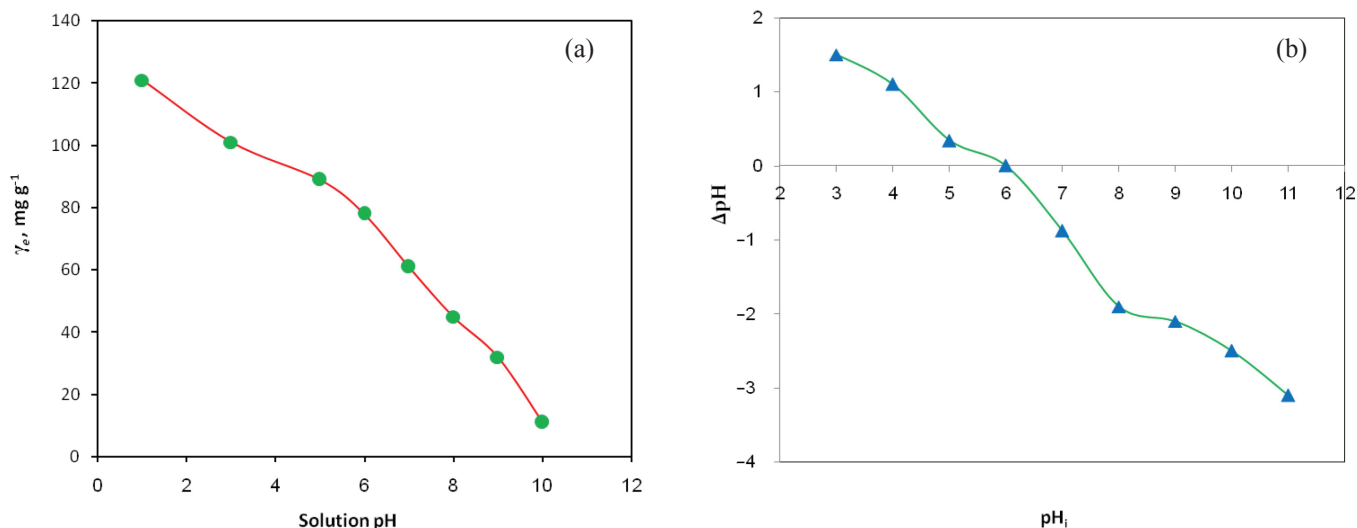


Fig. 11 – Effect of solution pH on Cr(VI) adsorption capacity of MHN adsorbent (a) and plot of ΔpH against pH_i of MHN adsorbent (b)

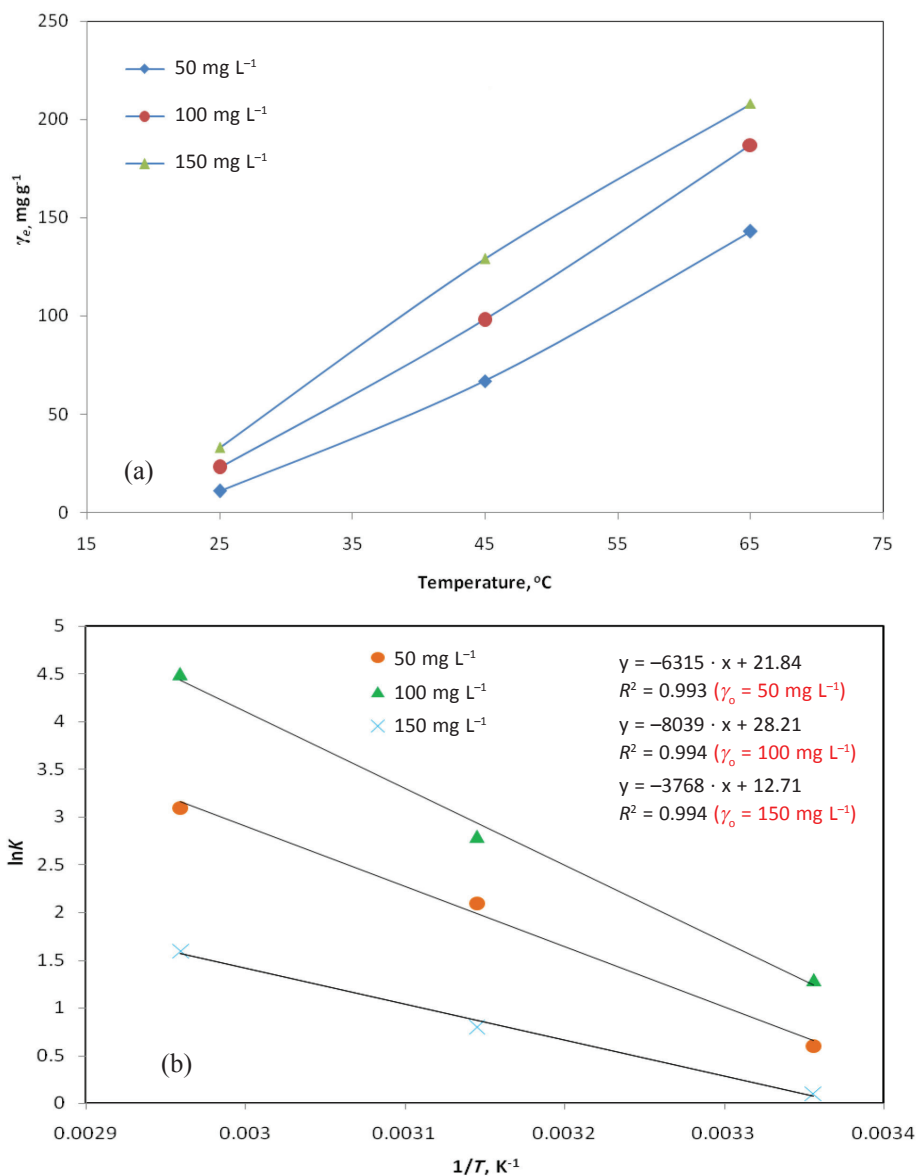


Fig. 12 – Effect of temperature on Cr(VI) adsorption (a) and plot of $\ln K$ versus $1/T$ (b)

Table 2 – Thermodynamic parameters for the adsorption of Cr(VI) onto the MHN adsorbent

q_0 (mg L ⁻¹)	ΔH° (kJ mol ⁻¹)	ΔS° (J K ⁻¹ mol ⁻¹)	ΔG° (kJ mol ⁻¹)		
			298 K	318 K	338 K
50	52.51	181.58	-19.38	-25.05	-38.66
100	66.84	234.54	-22.82	-32.66	-39.91
150	31.33	105.67	-37.29	-44.21	-61.33

Table 3 – Comparison of sorption capacity of Cr(VI) on various adsorbents

Adsorbent	Adsorption capacity (mg g ⁻¹)	Reference
Poly(Py)/glycine	217	[1]
PANi/Humic acid	150	[51]
Poly(Py)/MWCNT	294	[14]
Bi ₂ O ₃ nanotubes	79	[64]
Poly(Py)/attapulgitite	48	[65]
Poly(Py)/chitosan	78	[66]
Poly(Py)/cellulose fiber	13	[67]
Poly(Py) nanocomposite	169	[12]
Hydrous zirconium oxide	61	[68]
Activated carbon	15	[69]
Carboxylated chitosan beads	4	[70]
MHN adsorbent	208	This work

As important factors in the design of adsorption process, the thermodynamic parameters including the change in enthalpy (ΔH°), entropy (ΔS°), and free energy (ΔG°), were obtained from the following equations:

$$\ln K = \frac{\Delta S^\circ}{R} - \frac{\Delta H^\circ}{RT} \quad (3)$$

$$\Delta G^\circ = \Delta H^\circ - T\Delta S^\circ \quad (4)$$

where K is adsorption affinity, R is the gas constant (8.314 J mol⁻¹ K⁻¹), and T is the temperature in Kelvin. A linear plot of $\ln K$ versus $1/T$ (Fig. 12(b)) was employed, and the values of ΔH° and ΔS° were obtained from the slope and intercept, respectively. The ΔG° values were then calculated from Eq. (4). For all concentrations of Cr(VI), the values of ΔG° were negative in the adsorption process (Table 2), suggesting that the adsorption was favorable from a thermodynamic point of view and spontaneous in nature. It is worth noticing that the ΔH° and ΔS° with positive values demonstrated that the ion adsorption process was endothermic and favorable.

After optimizing the ion adsorption capacity of the synthesized MHN adsorbent, it was found that the Cr(VI) adsorption amount by synthesized adsorbent was 208 mg g⁻¹, which was highly comparable to those mentioned previously for other chromium adsorbents (Table 3). In conclusion, the as-prepared adsorbent with acceptable adsorption capacity can be utilized as an ideal material for wastewater treatment.

Conclusions

In the present work, a novel magnetic superabsorbent hydrogel nanocomposite has been synthesized, and successfully utilized as efficient adsorbent for the removal of toxic Cr(VI) ion from aqueous solutions. Nanocomposites can be separated easily from wastewaters by applying an external magnet due to the superparamagnetic property of the synthesized adsorbents. The experimental results showed that the adsorbent capacity was mainly dependent on Fe₃O₄ content, monomer concentration, initial pH of solution, and temperature. The sorption data also indicated that the maximum Cr(VI) adsorption value was 208 mg g⁻¹. Further, thermodynamic studies demonstrated that the adsorption process of Cr(VI) by MHNs was endothermic and spontaneous in nature. In conclusion, it is expected that the MHNs could be regarded as highly effective adsorbent materials for cleaning various metal ions from wastewaters.

References

- Ballav, D., Maity, A., Mishra, S. B., High efficient removal of chromium(VI) using glycine doped polypyrrole adsorbent from aqueous solution, *Chem. Eng. J.* **198** (2012) 536. doi: <https://doi.org/10.1016/j.cej.2012.05.110>
- Zhang, L. D., Fang, M., Nanomaterials in pollution trace detection and environmental improvement, *Nano Today* **5** (2012) 128. doi: <https://doi.org/10.1016/j.nantod.2010.03.002>
- Tofighy, M. A., Mohammadi, T., Adsorption of divalent heavy metal ions from water using carbon nanotube sheets, *J. Hazard. Mater.* **185** (2011) 140. doi: <https://doi.org/10.1016/j.jhazmat.2010.09.008>
- Testa, J. J., Grela, M. A., Litter, M. I., Heterogeneous photocatalytic reduction of chromium(VI) over TiO₂ particle in presence of oxalate: Involvement of Cr(VI) species, *Environ. Sci. Technol.* **38** (2004) 1589. doi: <https://doi.org/10.1021/es0346532>
- Yao, X., Deng, S., Wu, R., Hong, S., Wang, B., Huang, J., Wang, Y., Yua, G., Highly efficient removal of hexavalent chromium from electroplating wastewater using aminated wheat straw, *RSC Adv.* **6** (2016) 8797. doi: <https://doi.org/10.1039/C5RA24508G>
- Huang, B., Liu, Y., Li, B., Zeng, G., Hu, X., Zheng, B., Li, T., Jiang, L., Tan, X., Zhou, L., Synthesis of graphene oxide decorated with core@double-shell nanoparticles and application for Cr(VI) removal, *RSC Adv.* **5** (2015) 106339. doi: <https://doi.org/10.1039/C5RA22862J>

7. EPA (Environmental Protection Agency), Environmental Pollution Control Alternatives, EPA/625/5-90/025, EPA/625/4-89/023, Cincinnati, US, 1990.
8. Singh, P. N., Tiwary, D., Sinha, L., Chromium removal from aqueous media by superparamagnetic starch functionalized maghemite nanoparticles, *J. Chem. Sci.* **127** (2015) 1967.
doi: <https://doi.org/10.1007/s12039-015-0957-0>
9. Prabhakaran, S. K., Vijayaraghavan, K., Balasubramanian, R., Removal of Cr(VI) ions by spent tea and coffee dusts: Reduction to Cr(III) and biosorption, *Ind. Eng. Chem. Res.* **48** (2009) 2113.
doi: <https://doi.org/10.1021/ie801380h>
10. Bayramoglu, G., Arica, M. Y., Synthesis of Cr(VI)-imprinted poly(4-vinyl pyridine co-hydroxyethyl methacrylate) particles: Its adsorption propensity to Cr(VI), *J. Hazard. Mater.* **187** (2011) 213.
doi: <https://doi.org/10.1016/j.jhazmat.2011.01.022>
11. Liu, B., Huang, Y., Polyethyleneimine modified eggshell membrane as a novel biosorbent for adsorption and detoxification of Cr(VI) from water, *J. Mater. Chem.* **21** (2011) 17413.
doi: <https://doi.org/10.1039/c1jm12329g>
12. Wang, Y. Q., Zou, B. F., Gao, T., Wu, X. P., Lou, S. Y., Zhou, S. M., Synthesis of orange-like Fe₃O₄/PPy composite microspheres and their excellent Cr(VI) ion removal properties, *J. Mater. Chem.* **22** (2012) 9034.
doi: <https://doi.org/10.1039/c2jm30440f>
13. Bhaumik, M., Maity, A., Srinivasu, V. V., Onyango, M. S., Enhanced removal of Cr(VI) from aqueous solution using polypyrrole/Fe₃O₄ magnetic nanocomposite, *J. Hazard. Mater.* **190** (2011) 381.
doi: <https://doi.org/10.1016/j.jhazmat.2011.03.062>
14. Bajpai, S. K., Rohit, V. K., Removal of hexavalent chromium from aqueous solution by sorption into a novel sawdust anion exchanger (SAE) sorbent, *J. Environ. Prot. Sci.* **3** (2009) 23.
15. Rengaraj, S., Joo, C. K., Kim, Y., Yi, J., Kinetics of removal of chromium from water and electronic process wastewater by ion exchange resins: 1200H, 1500H and IRN97H, *J. Hazard. Mater.* **102** (2003) 257.
doi: [https://doi.org/10.1016/S0304-3894\(03\)00209-7](https://doi.org/10.1016/S0304-3894(03)00209-7)
16. Kozłowski, C. A., Walkowiak, W., Removal of Cr(VI) from aqueous solution by polymer inclusion membranes, *Water Res.* **36** (2002) 4870.
doi: [https://doi.org/10.1016/S0043-1354\(02\)00216-6](https://doi.org/10.1016/S0043-1354(02)00216-6)
17. Pugazhenthii, G., Sachan, S., Kishore, N., Kumar, A., Separation of chromium (VI) using modified ultrafiltration charged carbon membrane and its mathematical modeling, *J. Membr. Sci.* **254** (2005) 229.
doi: <https://doi.org/10.1016/j.memsci.2005.01.011>
18. Animes, K. G., Ajoy, K. C., Amar, N. S., Subhabrata, R., Removal of Cr(VI) from aqueous solution: Electrocoagulation vs chemical coagulation, *Sep. Sci. Technol.* **42** (2007) 2177.
doi: <https://doi.org/10.1080/01496390701446464>
19. Bhatti, M. S., Reddy, A. S., Thukral, A. K., Electrocoagulation removal of Cr(VI) from simulated wastewater using response surface methodology, *J. Hazard. Mater.* **172** (2009) 839.
doi: <https://doi.org/10.1016/j.jhazmat.2009.07.072>
20. Olmez, T., The optimization of Cr(VI) reduction and removal by electrocoagulation using response surface methodology, *J. Hazard. Mater.* **162** (2009) 1371.
doi: <https://doi.org/10.1016/j.jhazmat.2008.06.017>
21. Liu, Y., Yuan, D., Yan, J., Li, Q., Ouyang, T., Electrochemical removal of chromium from aqueous solutions using electrodes of stainless steel nets coated with single wall carbon nanotubes, *J. Hazard. Mater.* **186** (2011) 473.
doi: <https://doi.org/10.1016/j.jhazmat.2010.11.025>
22. Tian, Y., Yang, F., Reduction of hexavalent chromium by polypyrrole-modified steel mesh electrode, *J. Cleaner Prod.* **15** (2007) 1415.
doi: <https://doi.org/10.1016/j.jclepro.2006.04.001>
23. Golder, A. K., Chanda, A. K., Samanta, A. N., Ray, S., Removal of hexavalent chromium by electrochemical reduction–precipitation: Investigation of process performance and reaction stoichiometry, *Sep. Purif. Technol.* **76** (2010) 345.
doi: <https://doi.org/10.1016/j.seppur.2010.11.002>
24. Bhattagar, A., Sillanpaa, M., Utilization of agro-industrial and municipal waste materials as potential adsorbents for water treatment-A review, *Chem. Eng. J.* **157** (2010) 277.
doi: <https://doi.org/10.1016/j.cej.2010.01.007>
25. Park, H. J., Tavlarides, L. L., Adsorption of chromium (VI) from aqueous solution using an imidazole functionalized adsorbent, *Ind. Eng. Chem. Res.* **47** (2008) 3401.
doi: [https://doi.org/10.1016/0043-1354\(95\)00035-J](https://doi.org/10.1016/0043-1354(95)00035-J)
26. Manuel, P. C., Jose, M. M., Rosa, T. M., Chromium (VI) removal with activated carbons, *Water Res.* **29** (1995) 2174.
doi: [https://doi.org/10.1016/0043-1354\(95\)00035-J](https://doi.org/10.1016/0043-1354(95)00035-J)
27. Mohan, D., Sing, K. P., Sing, V. K., Removal of hexavalent chromium from aqueous solution using low cost activated carbon derived from agricultural waste materials and activated carbon fabric cloth, *Ind. Eng. Chem. Res.* **44** (2005) 1027.
doi: <https://doi.org/10.1021/ie0400898>
28. Goshu, V., Tsarev, Y. V., Kastrov, V. V., Russ kinetics of chromium (VI) adsorption from model solutions on iron oxide, *Russ. J. Appl. Chem.* **82** (2009) 801.
doi: <https://doi.org/10.1134/S1070427209050097>
29. Gang, D., Hu, W., Banerji, S. K., Clevenger, T. E., Modified poly-(4-vinylpyridine)coated silica gel. Fast kinetics of diffusion-controlled sorption of chromium(VI), *Ind. Eng. Chem. Res.* **40** (2001) 1200.
doi: <https://doi.org/10.1021/ie000771b>
30. Cong, H. P., Ren, X. C., Wang, P., Yu, S. H., Macroscopic multifunctional graphene-based hydrogels and aerogels by a metal ion induced self-assembly process, *ACS Nano* **6** (2012) 2693.
doi: <https://doi.org/10.1021/nn300082k>
31. Banarjee, S. S., Joshi, M. V., Jayaram, R. V., Removal of Cr(VI) and Hg(II) from aqueous solutions using fly ash and impregnated fly ash, *Sep. Sci. Technol.* **39** (2004) 1611.
doi: <https://doi.org/10.1081/SS-120030778>
32. Wang, S., Wei, M., Hunag, Y., Biosorption of multifold toxic heavy metal ions from aqueous water onto food residue eggshell membrane functionalized with ammonium thioglycolate, *J. Agric. Food Chem.* **61** (2013) 4988.
doi: <https://doi.org/10.1021/jf4003939>
33. Chand, R., Narimura, K., Kawakita, H., Ohto, K., Watari, T., Inoue, K., Grape waste as a biosorbent for removing Cr(VI) from aqueous solution, *J. Hazard. Mater.* **163** (2009) 245.
doi: <https://doi.org/10.1016/j.jhazmat.2008.06.084>
34. Yu, Z., Zhang, X., Huang, Y., Magnetic chitosan–iron(III) hydrogel as a fast and reusable adsorbent for chromium(VI) removal, *Ind. Eng. Chem. Res.* **52** (2013) 11956.
doi: <https://doi.org/10.1021/ie400781n>

35. *Boddu, V. M., Abburi, K., Talbott, J. L., Smith, E. D.*, Removal of hexavalent chromium from wastewater using a new composite chitosan biosorbent, *Environ. Sci. Technol.* **37** (2003) 4449.
doi: <https://doi.org/10.1021/es021013a>
36. *Hu, J., Chen, G. H., Lo, I. M. C.*, Removal and recovery of Cr(VI) from wastewater by maghemite nanoparticles, *Water Res.* **39** (2005) 4528.
doi: <https://doi.org/10.1016/j.watres.2005.05.051>
37. *Zhao, X., Shi, Y., Cai, Y., Mou, S.*, Cetyltrimethylammonium bromide coated magnetic nanoparticles for the preconcentration of phenolic compounds from environmental water samples, *Environ. Sci. Technol.* **42** (2008) 1201.
doi: <https://doi.org/10.1021/es071817w>
38. *Hu, J., Lo, I. M. C., Chen, Y.*, Removal of Cr(VI) by magnetite, *Water Sci. Technol.* **50** (2004) 139.
doi: <https://doi.org/10.2166/wst.2004.0706>
39. *Xiao, Z. H., Zhang, R., Chen, X. Y., Li, X. L., Zhou, T. F.*, Magnetically recoverable Ni@carbon nanocomposites: Solid-state synthesis and the application as excellent adsorbents for heavy metal ions, *Appl. Surf. Sci.* **263** (2012) 795.
doi: <https://doi.org/10.1016/j.apsusc.2012.09.175>
40. *Debrassi, A., Correa, A. F., Baccarin, T., Nedelko, N., Slawska-Waniewska, A., Sobczak, K., Dłuzewski, P., Greneche, G. M., Rodrigues, C. A.*, Removal of cationic dyes from aqueous solutions using N-benzyl-O-carboxymethylchitosan magnetic nanoparticles, *Chem. Eng. J.* **183** (2012) 284.
doi: <https://doi.org/10.1016/j.cej.2011.12.078>
41. *Dayyani, N., Ramazani, A., Khoee, S., Shafiee, A.*, Synthesis and characterization of the first generation of polyamino-ester dendrimer-grafted magnetite nanoparticles from 3-aminopropyltriethoxysilane (APTES) via the convergent approach, *Silicon* **10** (2018) 595.
doi: <https://doi.org/10.1007/s12633-016-9497-6>
42. *Gutha, Y., Zhang, Y., Zhang, W., Jiao, X.*, Magnetic-epichlorohydrin crosslinked chitosan schiff's base (m-ECCSB) as a novel adsorbent for the removal of Cu(II) ions from aqueous environment, *Int. J. Biolog. Macromol.* **97** (2017) 85.
doi: <https://doi.org/10.1016/j.ijbiomac.2017.01.004>
43. *Li, X., Liu, Y., Zhang, C., Wen, T., Zhuang, L., Wang, X., Song, G., Chen, D., Ai, Y., Hayat, T., Wang, X.*, Porous Fe₂O₃ microcubes derived from metal organic frameworks for efficient elimination of organic pollutants and heavy metal ions, *Chem. Eng. J.* **336** (2018) 241.
doi: <https://doi.org/10.1016/j.cej.2017.11.188>
44. *Sahraei, R., Sekhavat Pour, Z., Ghaemy, M.*, Novel magnetic bio-sorbent hydrogel beads based on modified gum tragacanth/graphene oxide: Removal of heavy metals and dyes from water, *J. Cleaner Prod.* **142** (2017) 2973.
doi: <https://doi.org/10.1016/j.jclepro.2016.10.170>
45. *Bhaumik, M., Agarwal, S., Gupta, V. K., Maity, A.*, Kinetics of removal of chromium from water and electronic process wastewater by ion exchange resins: 1200H, 1500H and IRN97H, *J. Colloid Interf. Sci.* **470** (2016) 257.
doi: <https://doi.org/10.1016/j.jcis.2016.02.054>
46. *Chen, J., Shu, C., Wang, N., Feng, J., Ma, H., Yan, W.*, Adsorbent synthesis of polypyrrole/TiO₂ for effective fluoride removal from aqueous solution for drinking water purification: Adsorbent characterization and adsorption mechanism, *J. Colloid Interf. Sci.* **495** (2017) 44.
doi: <https://doi.org/10.1016/j.jcis.2017.01.084>
47. *Liu, Q., Zhu, J., Tan, L., Jing, X., Liu, J., Song, D., Zhang, H., Li, R., Emelchenko, J. A., Wang, J.*, Polypyrrole/cobalt ferrite/multiwalled carbon nanotubes as an adsorbent for removing uranium ions from aqueous solutions, *J. Dalton Trans.* **45** (2016) 9166.
doi: <https://doi.org/10.1039/C6DT00912C>
48. *Guo, X., Fei, G. T., Su, H., Zhang, L. D.*, Comparison of ab Initio, DFT, and semiempirical QM/MM approaches for description of catalytic mechanism of hairpin ribozyme, *J. Phys. Chem. B* **115** (2011) 1608.
49. *Bhaumik, M., Maity, A., Srinivasu, V. V., Onyango, M. S.*, Removal of hexavalent chromium from aqueous solution using polypyrrole-polyaniline nanofibers, *Chem. Eng. J.* **181** (2012) 323.
doi: <https://doi.org/10.1016/j.cej.2011.11.088>
50. *Li, Q., Sun, L., Zhang, Y., Qian, Y., Zhai, J.*, Characteristics of equilibrium, kinetics studies for adsorption of Hg(II) and Cr(VI) by polyaniline/humic acid composite, *Desalination* **266** (2011) 188.
doi: <https://doi.org/10.1016/j.desal.2010.08.025>
51. *Katal, R., Ghiass, M., Estandian, H.*, Application of nanometer size of polypyrrole as a suitable adsorbent for removal of Cr(VI), *Vinyl Addit. V. Technol.* **17** (2011) 222.
52. *Lu, X., Zhang, W., Wang, C., Wen, T. C., Wei, Y.*, One-dimensional conducting polymer nanocomposites: Synthesis, properties and applications, *Prog. Polym. Sci.* **36** (2011) 671.
doi: <https://doi.org/10.1016/j.progpolymsci.2010.07.010>
53. *Lee, H. T., Liu, Y. C., Lin, L. H.*, Characteristics of polypyrrole electrodeposited onto roughened substrates composed of gold-silver bimetallic nanoparticle, *J. Polym. Sci. A Polym. Chem.* **44** (2006) 2724.
doi: <https://doi.org/10.1002/pola.21385>
54. *Zhang, X., Bai, R. B., Tong, Y. W.*, Selective adsorption behaviors of proteins on polypyrrole-based adsorbents, *Sep. Purif. Technol.* **52** (2006) 161.
doi: <https://doi.org/10.1016/j.seppur.2006.04.001>
55. *Bajpai, S. K., Rohit, V. K., Namdeo, M.*, Removal of phosphate anions from aqueous solutions using polypyrrole-coated sawdust as a novel sorbent, *J. Appl. Polym. Sci.* **111** (2009) 3081.
doi: <https://doi.org/10.1002/app.29363>
56. *Pan, B., Gao, F., Gu, H.*, Dendrimer modified magnetite nanoparticles for protein immobilization, *J. Colloid Interface Sci.* **284** (2005) 1.
doi: <https://doi.org/10.1016/j.jcis.2004.09.073>
57. *Sun, H., Cao, L., Lu, L.*, Magnetite/reduced graphene oxide nanocomposites: One step solvothermal synthesis and use as a novel platform for removal of dye pollutants, *Nano Res.* **4** (2011) 550.
doi: <https://doi.org/10.1007/s12274-011-0111-3>
58. *Schild, H. G.*, Thermal decomposition of PNIPAAm: TGA-FTIR analysis, *J. Polym. Sci. Part A: Polym. Chem.* **34** (1996) 2259.
doi: [https://doi.org/10.1002/\(SICI\)1099-0518\(199608\)34:11<2259::AID-POLA21>3.0.CO;2-D](https://doi.org/10.1002/(SICI)1099-0518(199608)34:11<2259::AID-POLA21>3.0.CO;2-D)
59. *Zeinali, E., Haddadi-Asl, V., Roghani-Mamaqani, H.*, Nanocrystalline cellulose grafted random copolymers of N-isopropylacrylamide and acrylic acid synthesized by RAFT polymerization: Effect of different acrylic acid contents on LCST behavior, *RSC Adv.* **4** (2014) 31428.
doi: <https://doi.org/10.1039/C4RA05442C>
60. *Dayyani, N., Ramazani, A., Khoee, S., Shafiee, A.*, Synthesis and characterization of the first generation of polyamino-ester dendrimer-grafted magnetite nanoparticles from 3-aminopropyltriethoxysilane (APTES) via the convergent approach, *Silicon* **10** (2018) 595.
doi: <https://doi.org/10.1007/s12633-016-9497-6>
61. *Peppas, L. B., Harland, R. S.*, *Absorbent Polymer Technology*, Elsevier, Amsterdam, 1990, pp 103-106.
62. *Buchholz, F. L., Graham, A. T.*, *Modern Superabsorbent Polymer Technology*, Wiley, New York, 1997, pp 309–323.

63. Huang, S. H., Liao, M. H., Chen, D. H., Direct binding and characterization of lipase onto magnetic nanoparticles, *Biotechnol. Prog.* **19** (2003) 1095.
doi: <https://doi.org/10.1021/bp025587v>
64. Qin, F., Li, G., Wang, R., Wu, J., Sun, H., Chen, R., Template-free fabrication of Bi₂O₃ and (BiO)₂CO₃ nanotubes and their application in water treatment, *Chem. Eur. J.* **18** (2012) 16491.
doi: <https://doi.org/10.1002/chem.201201989>
65. Chen, Y., Xu, H., Wang, S., Kang, L., Removal of Cr(VI) from water using polypyrrole/attapulgite core-shell nanocomposites: Equilibrium, thermodynamics and kinetics, *RSC Adv.* **4** (2014) 17805.
doi: <https://doi.org/10.1039/C3RA47351A>
66. Karthik, R., Meenakshi, S., Removal of hexavalent chromium ions from aqueous solution using chitosan/polypyrrole composite, *Desal. Water Treat.* **56** (2015) 1587.
doi: <https://doi.org/10.1080/19443994.2014.951964>
67. Lei, Y., Qian, X., Shen, J., An, X., Adsorption of Cr(VI) from aqueous solution by hydrous zirconium oxide, *Ind. Eng. Chem. Res.* **51** (2012) 10408.
doi: <https://doi.org/10.1021/ie301136g>
68. Rodrigues, L. A., Maschio, L. J., Silva, R. A., Pinto da Silva, M. I. C., Adsorption of Cr(VI) from aqueous solution by hydrous zirconium oxide, *J. Hazard. Mater.* **173** (2010) 630.
doi: <https://doi.org/10.1016/j.jhazmat.2009.08.131>
69. Sandhya, B., Tonni, A. K., Cr(VI) removal from synthetic wastewater using coconut shell charcoal and commercial activated carbon modified with oxidizing agents and/or chitosan, *Chemosphere* **54** (2004) 951.
doi: <https://doi.org/10.1016/j.chemosphere.2003.10.001>
70. Kousalya, G. N., Rajiv Gandhi, M., Meenakshi, S., Removal of phosphate anions from aqueous solutions using polypyrrole-coated sawdust as a novel sorbent, *Int. J. Biol. Macromol.* **47** (2010) 308.
doi: <https://doi.org/10.1016/j.ijbiomac.2010.03.010>